Supplementary Methods

Imagestream® analysis

$CD8^+$ T cells were negatively enriched from PBMCs using EasySep^{TM} $CD8^+$ T cell separation kit (StemCell Technologies) and stained with anti-CD161 APC together with anti-CD107α FITC, anti-Granzyme A PerCP-Cy5.5 or anti-Granzyme K FITC. Cells were fixed before analysis by flow cytometry and image capture with Imagestream® imaging cytometer (Amnis Corporation). 15,000 events were collected on the Imagestream® for co-localisation analysis. Post-acquisition spectral compensation and statistical co-localisation analysis was performed using IDEAS® image analysis software package (Amnis Corporation).

Co-localisation was quantified using a 'Bright Detail Similarity Score', defined as a log-transformed Pearson's correlation coefficient of the intensities of the spatially correlated pixels within the whole cell, as a measure of the degree to which two images were linearly correlated. A score of >2.0 was considered co-localised.

In vitro stimulation (continued)

For profiling of granule contents after direct cytokine stimulation of $CD8^+$ T cells, $CD8^+$ T cells isolated using CD8 Microbeads (Miltenyi Biotec) were stimulated for 16 hours with the following cytokines/mitogens: recombinant human IL-2 (Roche), IL-12, IL-18, IL-15, IL-23, TGFβ, IL-1β (all Miltenyi Biotec), IL-21, IL-7 (both PeproTech Inc) all at 50ng/ml; PMA (50ng/ml) and ionomycin (250ng/ml) (Sigma-Aldrich); anti-CD3/CD28/CD2-coated beads (Miltenyi Biotec). For time-course PBMC stimulations, *E. coli* was added at 10BpC or anti-CD3/CD28/CD2-coated

beads at a 1:1 ratio. To assay IFNγ production, THP1s were cultured with *E. coli* overnight as described previously[13] at 25 BpC, washed, and then PBMCs were added for 5 hours, with Brefeldin A (eBioscience; 3μg/ml) added after 1 hour of stimulation.

Supplementary Figure legends

Figure S1. GrA and GrK expression in cord blood $CD8^+$ T cells, and simultaneous analysis of cytotoxic-granule composition of adult peripheral blood MAIT cells. A) Frequency of GrA and GrK expressing cells in cord blood $CD8^+$ T cells according to CD161 expression levels. Representative plot and cumulative data for 6 donors is shown. Results shown as mean ± S.E.M, analyzed by repeated measures one way ANOVA, with Bonferroni's multiple comparisons test. B) Frequency of perforin expressing cells in adult peripheral blood $CD8^+$ T cells from healthy donors according to CD161 expression levels. Cumulative data for 12 healthy individuals is shown. Results shown as mean ± S.E.M, analyzed by repeated measures one way ANOVA, with Bonferroni's multiple comparisons test. *P<0.05, ****P<0.0001. C) Simultaneous analysis of cytotoxic-granule composition of $V\alpha7.2^+CD161^{++}CD8^+$ T cells (MAIT cells) in *ex vivo* adult peripheral blood, on the basis of GrA, GrB, GrK, and perforin expression. All the possible combinations of the different markers are shown on the *x*-axis of the graph, and the percentage of MAIT cells expressing each of these combinations are shown on the *y*-axis. Each dot represents a healthy donor (n=8). Data is summarized in the pie chart, with each slice corresponding to the average proportion of MAIT cells positive for the combinations of markers shown on the graph.

Figure S2. Changes in cytotoxic granule content of MAIT cells with cytokine- and TCR-stimulation. Enriched $CD8^+$ T cells were stimulated for 24 hours with the indicated cytokines, anti-CD3 or anti-CD3/CD28/CD2 coated beads, or PMA/ionomycin, and analyzed for expression of A) GrB (n=8) B) Perforin (n=8) C) GrK (n=10) D) GrA (n=10) in MAIT cells. Cumulative data (left) and representative staining for each marker from the same donor (right) is shown for GrB and perforin, and histograms for the indicated stimuli are shown for GrA and GrK. Results analyzed by repeated measures one-way ANOVA with Bonferroni's multiple comparisons test. E, F) Expression of E) granulysin (n=8) and F) intracellular FasL (n=5) in $CD8^+$ T cells after stimulation of PBMCs with *E. coli* or anti-CD3/CD28/CD2 beads for 24 hours. NK cells were used as a positive control for staining. Representative staining (left) and cumulative data (right) is shown. Bars indicate mean ± S.E.M. *P<0.05, **P<0.01, ***P<0.001.

Figure S3. Changes in the expression of GrB, CD69, CD161 and Vα7.2 in MAIT cells with increasing concentration of *E. coli*. Enriched $CD8^+$ T cells were stimulated overnight with THP1 cells pre-exposed to *E. coli* at the indicated BpCs or PMA/ionomycin. A) Representative plots showing GrB (top), CD69 (middle), and Vα7.2 (bottom) expression against CD161 from the same donor. In the bottom panel, the highly activated $CD69^{high}$ cells are overlaid in blue, and the numbers represent the percentages of the indicated populations within the CD8+ T cells. B) Cumulative data showing percentage of GrB^+ cells (left) and gMFI of CD69 (right) within $CD161^{++}CD8^+$ T cells. C) Frequency of $CD161^{++}CD8^+$ T cells within $CD8^+$ T cells. D) Frequency of the indicated populations within $CD8^+$ T cells. For all data, mean ± S.E.M are shown (n=5).

Figure S4. *E. coli*-stimulated MAIT cells have a higher cytotoxic capacity compared to *ex vivo* MAIT cells. A) Flow cytometry gating strategy used to analyze specific killing of target cells mediated by MAIT cells. BCL and T cell gates were based on wells with only BCLs or T cells. B) Frequency of $CD161^{++}CD8^{+}$ T cells within the $CD8^{+}$ T cells, in the same donors either *ex vivo* or stimulated with *E. coli* for 6 days. C) Percentage specific killing plotted against E:T adjusted for actual ratio of $CD161^{++}CD8^{+}$ T cells to $CFSE^{+}$ target cells in each well calculated from the expected ratio (See Materials and Methods). D) Trogocytosis of CFSE and CTV from the $CFSE^{+}$ *E. coli*-exposed BCL or CTV^{+} negative control BCL membranes onto $CD161^{++}CD8^{+}$ T cells. $CFSE^{+}$ *E. coli*-exposed BCL = Target cells, CTV^{+} negative control BCL = Neg cells.

Figure S5. $CD161^{++}CD8^{+}$ T cells, including the MAIT cells, proliferate in response to cytokines and TCR-stimulation. A) THP1 cells pre-exposed to *E. coli* and irradiated were used to stimulate enriched CTV-labeled $CD8^{+}$ T cells for 6 days, with or without anti-MR1 blocking antibody. Histogram gated on $V\alpha7.2^{+}$ $CD161^{++}CD8^{+}$ T cells. B) Downregulation of CD161 in MAIT cells with increasing rounds of cell division, both in enriched $CD8^{+}$ T cells (top) and PBMCs (bottom) in response to *E. coli*. Graph shows fold change in gMFI of CD161 in proliferating CD161+$V\alpha7.2^{+}$ $CD8^{+}$ T cells compared to non-dividing $CD161^{++}V\alpha7.2^{+}CD8^{+}$ T cells in the same well. C) CTV-labeled PBMCs were stimulated with PFA-fixed *E. coli* for 6 days and stained for CD8β. CD8β gating based on isotype control. Proliferation of CD8αβ and CD8αα MAIT cells in representative donor shown in histogram. D-G) PBMCs from healthy donors were CTV-labeled and cultured for 6 days with the indicated stimuli. D) Representative staining of $CD8^{+}$ T cells showing dilution of

CTV and E) CD69 expression in response to cytokines, according to CD161 expression levels. F) Frequency of $CD161^{++}$ and $CD161^{+}CD8^{+}$ T cells diluting CTV after stimulation with the indicated stimuli (n=5-11). $CD161^{-}CD8^{+}$ T cells were not included in the analysis as they include naïve T cells. Frequency of CTV^{low} cells in unstimulated cells was subtracted for each donor. G) Frequency of $CD161^{++}$ and $CD161^{+}$ $CD8^{+}$ T cells expressing CD69 after 6 days of culture with the indicated stimuli (n=5-11). Frequency of CD69 expression in unstimulated cells was subtracted for each donor. Significance is indicated for differences between $CD161^{++}$ and $CD161^{+}CD8^{+}$ T cells analyzed by a two-way ANOVA with Bonferroni's multiple comparisons test.

Figure S6. Activation of $CD8^{-}CD161^{++}$/MAIT cells by *E. coli*. A, B) Degranulation of $CD8^{-}$ T cells in the killing assays. Representative plots showing gating of *ex vivo* (A; upper panel) and *E. coli*-stimulated (lower panel) $CD8^{-}$ T cells in the killing assays, and their CD107α expression in wells with or without *E. coli*-exposed target cells. B) Cumulative data showing increase in $\%CD107\alpha^{+}$ cells in indicated $CD8^{-}$ T cell populations compared to wells with T cells only. Two-way ANOVA, with Bonferroni's multiple comparisons test (n=8). C, D) 5hr stimulation of PBMCs with *E. coli*-exposed THP1 cells, looking at IFNγ production from $CD8^{+}$, $CD4^{+}$, and double-negative (DN; $CD8^{-}CD4^{-}$) MAIT cells. Gating strategy (C) and representative plots showing IFNγ production from different MAIT cell subsets (D). One-way ANOVA, with Bonferroni's multiple comparisons test (n=9).

Figure S1

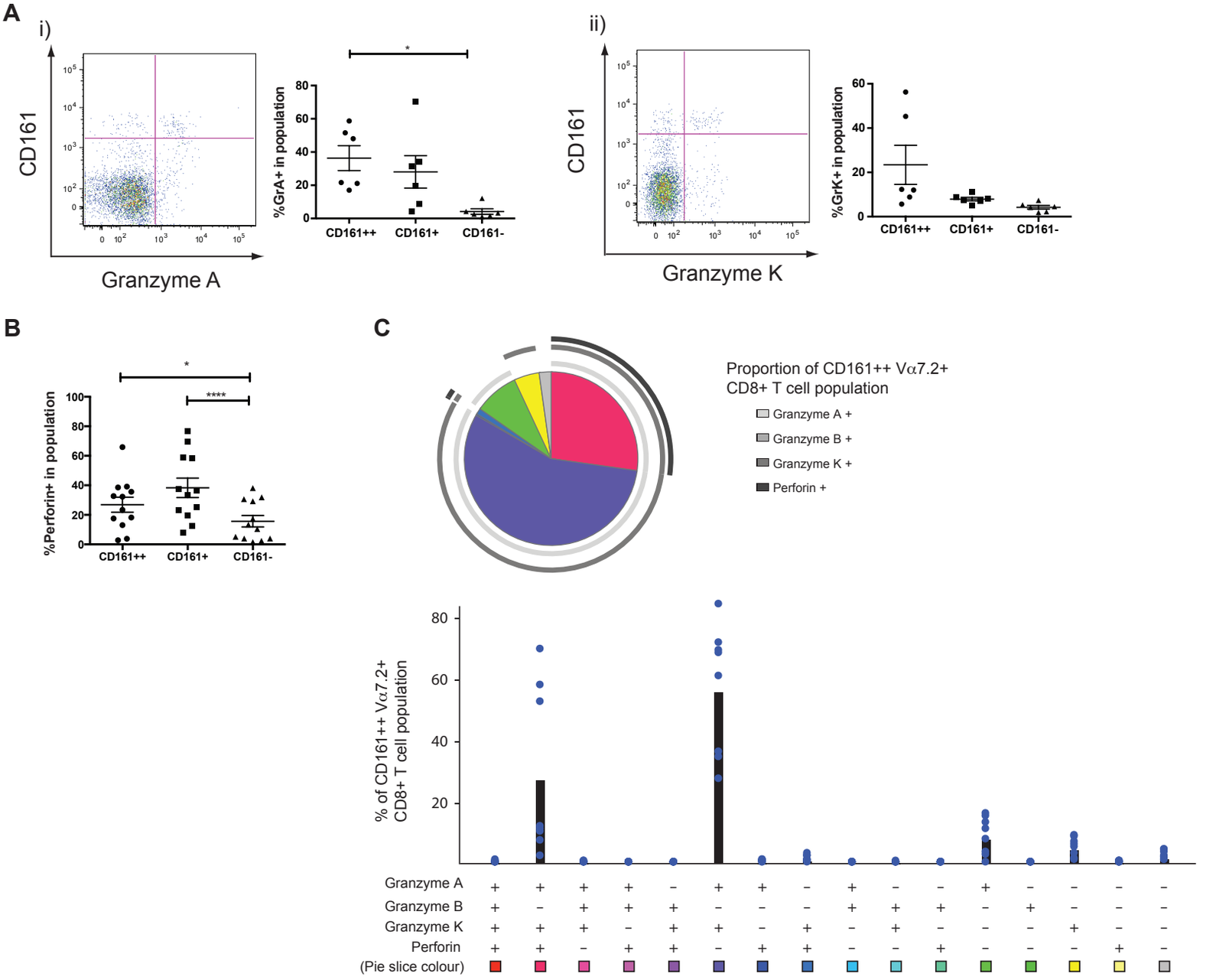
A
i)
CD161
Granzyme A
%GrA+ in population
CD161++
CD161+
CD161-
ii)
CD161
Granzyme K
%GrK+ in population
B
%Perforin+ in population
C
Proportion of CD161++ Vα7.2+ CD8+ T cell population
Granzyme A +
Granzyme B +
Granzyme K +
Perforin +
% of CD161++ Vα7.2+ CD8+ T cell population
Granzyme A
Granzyme B
Granzyme K
Perforin
(Pie slice colour)

Figure S2

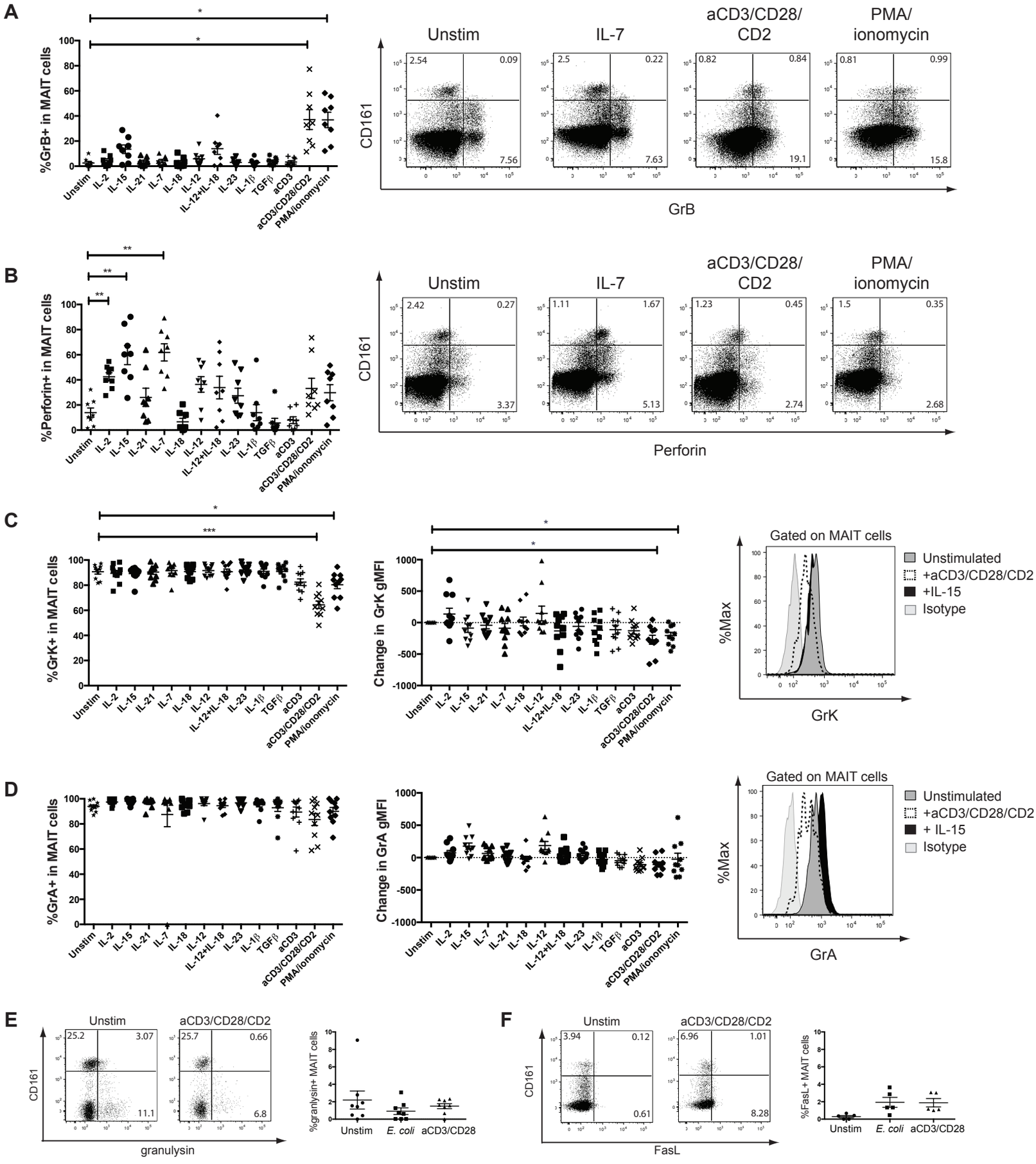
A
%GrB+ in MAIT cells
Unstim
IL-2
IL-15
IL-21
IL-7
IL-18
IL-12
IL-12+IL-18
IL-23
IL-1β
TGFβ
aCD3
aCD3/CD28/CD2
PMA/ionomycin
Unstim
IL-7
aCD3/CD28/ CD2
PMA/ ionomycin
CD161
GrB
2.54
0.09
7.56
2.5
0.22
7.63
0.82
0.84
19.1
0.81
0.99
15.8
B
%Perforin+ in MAIT cells
Perforin
2.42
0.27
3.37
1.11
1.67
5.13
1.23
0.45
2.74
1.5
0.35
2.68
C
%GrK+ in MAIT cells
Change in GrK gMFI
Gated on MAIT cells
%Max
GrK
Unstimulated
+aCD3/CD28/CD2
+IL-15
Isotype
D
%GrA+ in MAIT cells
Change in GrA gMFI
Gated on MAIT cells
%Max
GrA
Unstimulated
+aCD3/CD28/CD2
+ IL-15
Isotype
E
Unstim
aCD3/CD28/CD2
CD161
granulysin
25.2
3.07
11.1
25.7
0.66
6.8
%granlysin+ MAIT cells
Unstim
E. coli
aCD3/CD28
F
Unstim
aCD3/CD28/CD2
CD161
FasL
3.94
0.12
0.61
6.96
1.01
8.28
%FasL+ MAIT cells
Unstim
E. coli
aCD3/CD28

Figure S3

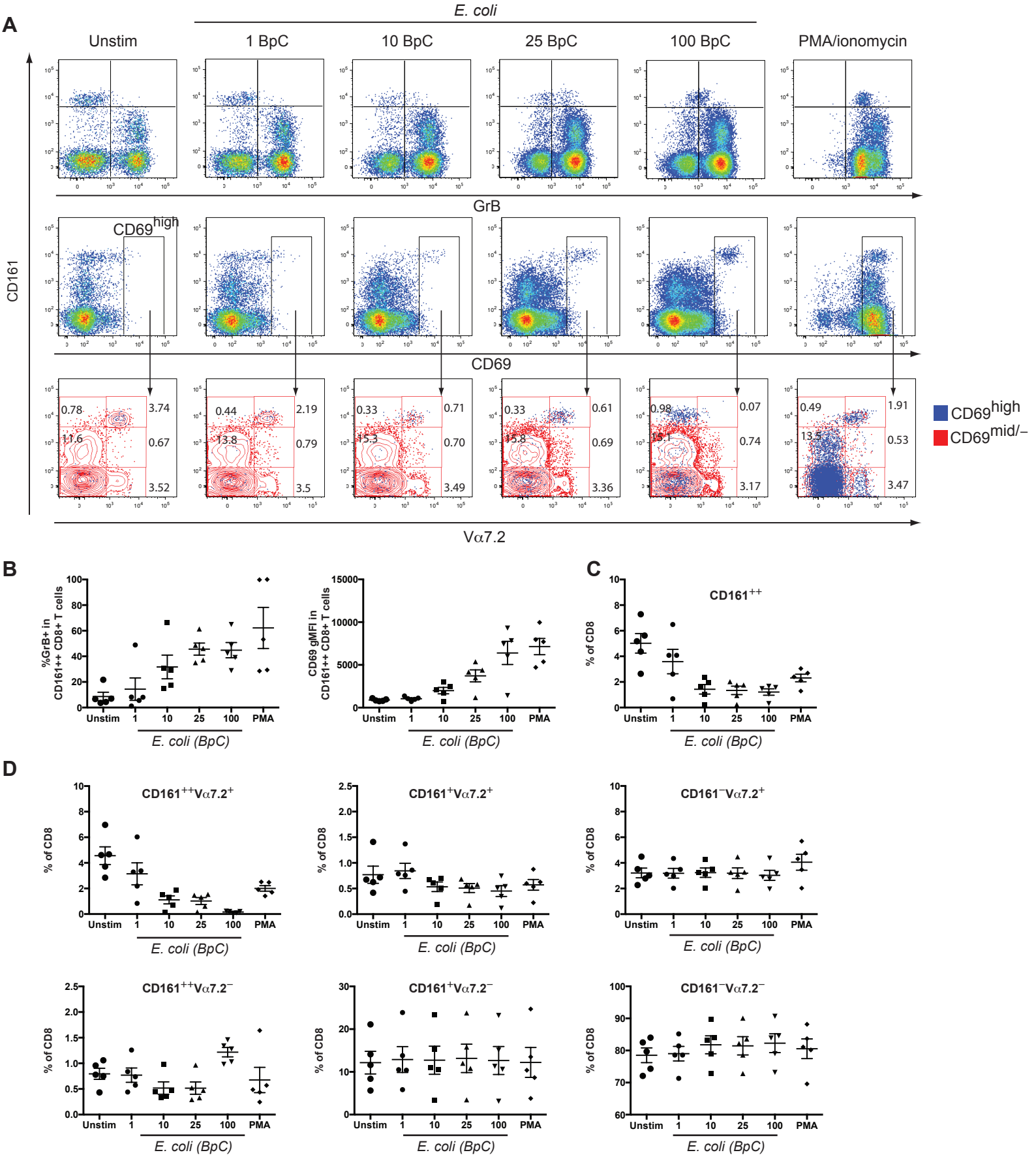
A
E. coli
Unstim
1 BpC
10 BpC
25 BpC
100 BpC
PMA/ionomycin
GrB
CD161
CD69high
CD69
Vα7.2
0.78
3.74
11.6
0.67
3.52
0.44
2.19
13.8
0.79
3.5
0.33
0.71
15.3
0.70
3.49
0.33
0.61
15.8
0.69
3.36
0.98
0.07
15.1
0.74
3.17
0.49
1.91
13.5
0.53
3.47
CD69high
CD69mid/−
B
%GrB+ in CD161++ CD8+ T cells
CD69 gMFI in CD161++ CD8+ T cells
Unstim
1
10
25
100
PMA
E. coli (BpC)
C
CD161++
% of CD8
D
CD161++Vα7.2+
CD161+Vα7.2+
CD161−Vα7.2+
CD161++Vα7.2−
CD161+Vα7.2−
CD161−Vα7.2−

Figure S4

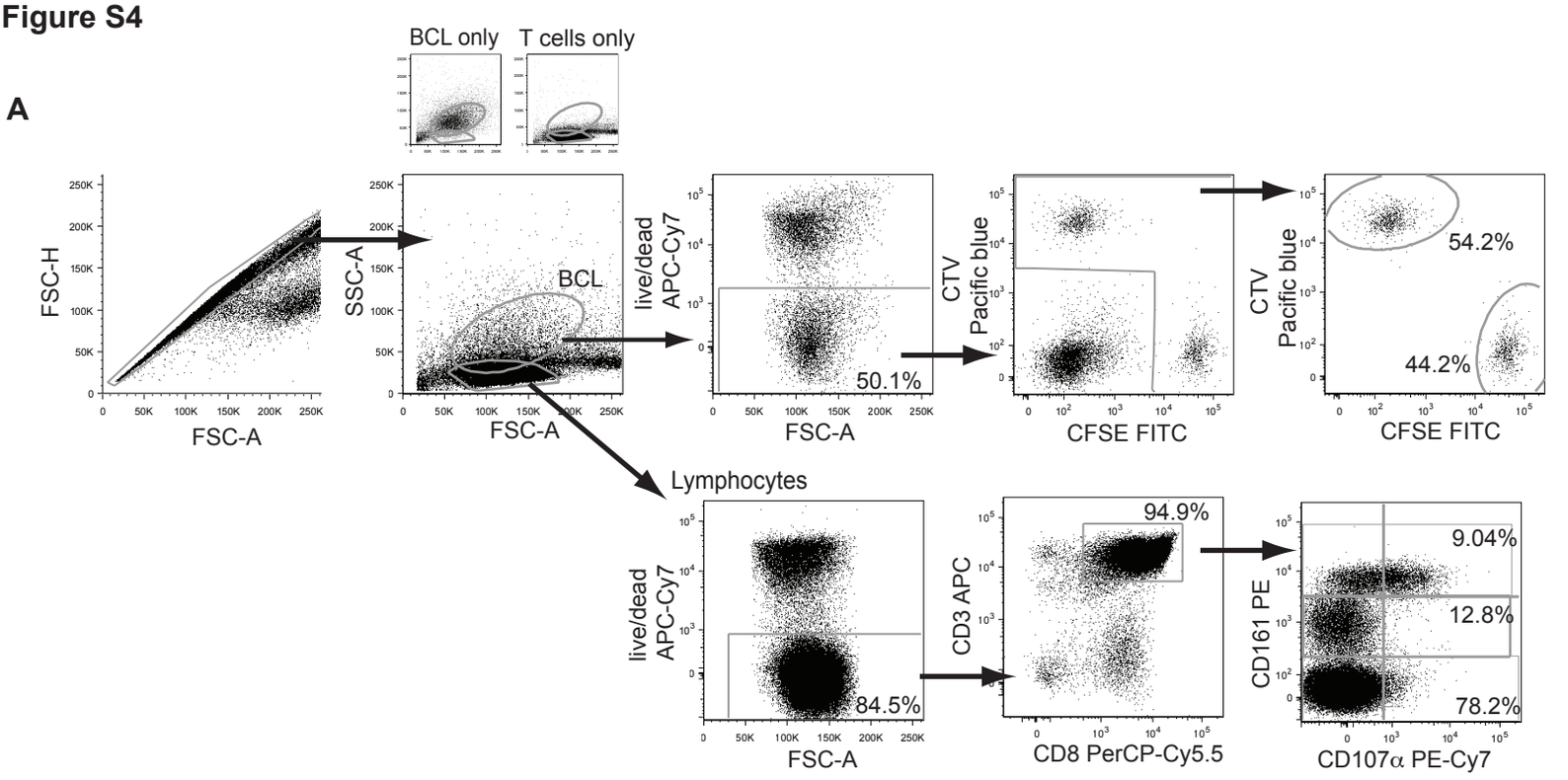
A
BCL only
T cells only
FSC-H
FSC-A
SSC-A
BCL
live/dead APC-Cy7
50.1%
CTV Pacific blue
CFSE FITC
54.2%
44.2%
Lymphocytes
84.5%
CD3 APC
94.9%
CD8 PerCP-Cy5.5
CD161 PE
9.04%
12.8%
78.2%
CD107α PE-Cy7

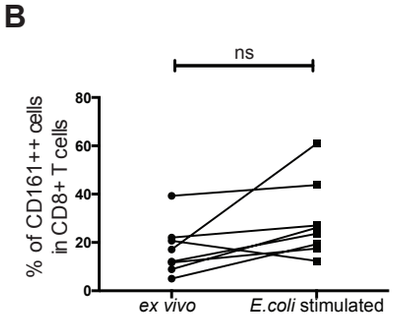
B
ns
% of CD161++ cells in CD8+ T cells
ex vivo
E.coli stimulated

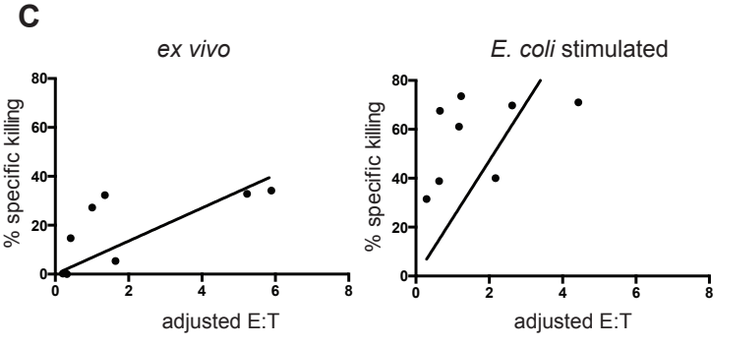
C
ex vivo
E. coli stimulated
% specific killing
adjusted E:T

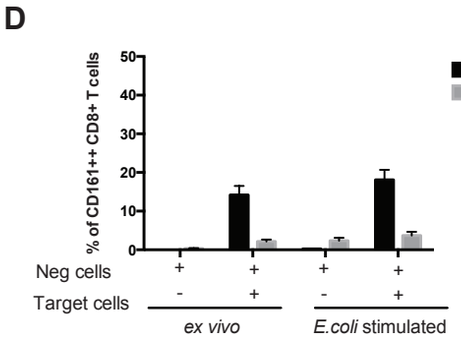
D
% of CD161++ CD8+ T cells
CFSE+
CTV+
Neg cells
Target cells
ex vivo
E.coli stimulated

Figure S5

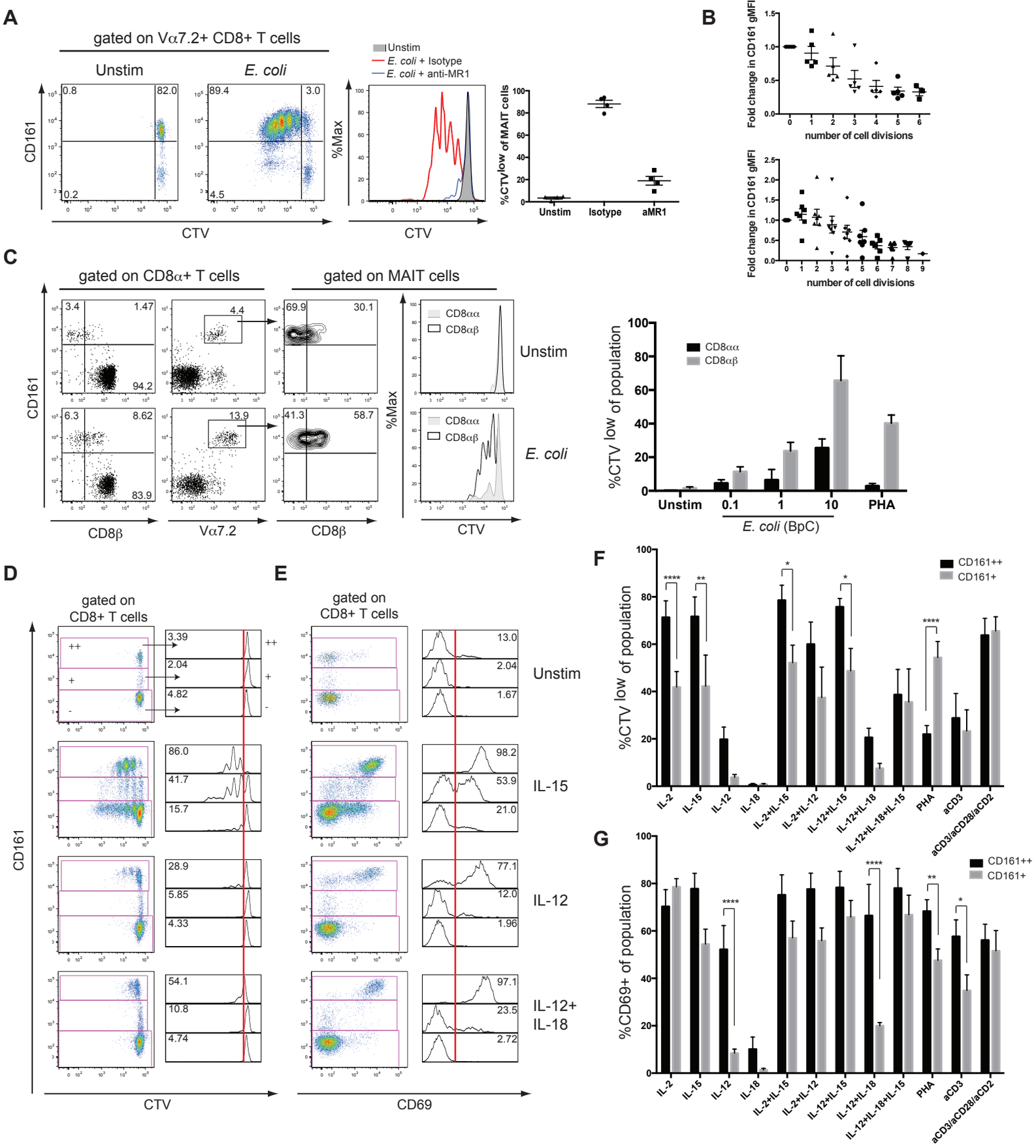
A
gated on Vα7.2+ CD8+ T cells
Unstim
E. coli
CD161
CTV
Unstim
E. coli + Isotype
E. coli + anti-MR1
%Max
%CTVlow of MAIT cells
Unstim
Isotype
aMR1
B
Fold change in CD161 gMFI
number of cell divisions
C
gated on CD8α+ T cells
gated on MAIT cells
CD8αα
CD8αβ
Unstim
E. coli
CD8β
Vα7.2
%CTV low of population
E. coli (BpC)
D
E
gated on CD8+ T cells
IL-15
IL-12
IL-12+ IL-18
CD69
F
CD161++
CD161+
%CTV low of population
IL-2
IL-15
IL-12
IL-18
IL-2+IL-15
IL-2+IL-12
IL-12+IL-15
IL-12+IL-18
IL-12+IL-18+IL-15
PHA
aCD3
aCD3/aCD28/aCD2
G
%CD69+ of population

Figure S6

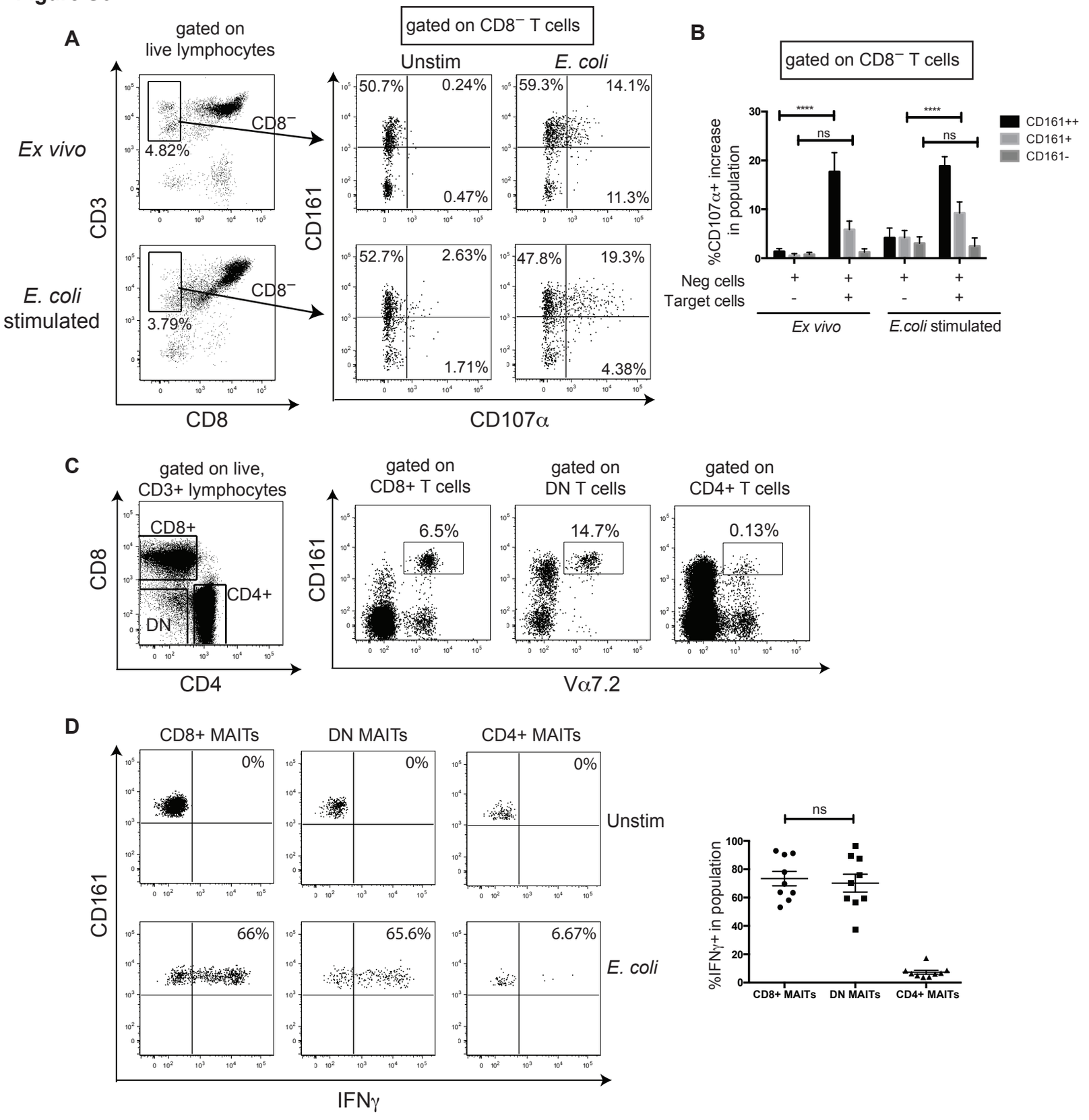
A
gated on live lymphocytes
gated on CD8⁻ T cells
Unstim
E. coli
Ex vivo
E. coli stimulated
CD8⁻
4.82%
3.79%
50.7%
0.24%
0.47%
59.3%
14.1%
11.3%
52.7%
2.63%
1.71%
47.8%
19.3%
4.38%
CD3
CD8
CD161
CD107α
B
gated on CD8⁻ T cells
%CD107α+ increase in population
****
ns
CD161++
CD161+
CD161-
Neg cells
Target cells
Ex vivo
E.coli stimulated
C
gated on live, CD3+ lymphocytes
gated on CD8+ T cells
gated on DN T cells
gated on CD4+ T cells
CD8+
CD4+
DN
6.5%
14.7%
0.13%
CD8
CD4
CD161
Vα7.2
D
CD8+ MAITs
DN MAITs
CD4+ MAITs
0%
Unstim
66%
65.6%
6.67%
E. coli
CD161
IFNγ
ns
%IFNγ+ in population
CD8+ MAITs
DN MAITs
CD4+ MAITs